Structural stability of the CO_2@sI hydrate: a bottom-up quantum chemistry approach on the guest-cage and inter-cage interactions

Adriana Cabrera-Ramírez* Daniel J. Arismendi-Arrieta†‡

Álvaro Valdés§ Rita Prosmiti*¶

September 30, 2020

1 Abstract

Through reliable first-principles computations, we have demonstrated the impact of CO_2 molecules enclathration on the stability of sI clathrate hydrates. Given the delicate balance between the interaction energy components (van der Waals, hydrogen bonds) present on such systems, we follow a systematic bottom-up approach starting from the individual 5^{12} and $5^{12}6^2$ sI cages, up to all existing combinations of two-adjacent sI crystal cages to evaluate how such clathrate-like models perform on the evaluation of the guest-host and first-neighbors inter-cage effects, respectively. Interaction and binding energies of the CO_2 occupation of the sI cages were computed using DF-MP2 and different DFT/DFT-D electronic structure methodologies. The performance of selected DFT functionals, together with various semi-classical dispersion corrections schemes, were validated by comparison with reference *ab initio* DF-MP2 data, as well as experimental data from x-ray and neutron diffraction studies available. Our investigation confirms that the inclusion of the CO_2 in the cage/s is an energetically favorable process, with the CO_2 molecule preferring to occupy the large $5^{12}6^2$ sI cages compared to the 5^{12} ones. Further, the present results conclude on the rigidity of the water cages arrangements, showing the importance of the inter-cage couplings in the cluster models under study. In particular, the guest-cage interaction is the key factor for the preferential orientation of the captured CO_2 molecules in the sI cages, while the inter-cage

*Institute of Fundamental Physics (IFF-CSIC), CSIC, Serrano 123, 28006 Madrid, Spain

†Corresponding author: darismendi@dipc.org

‡Donostia International Physics Center (DIPC), Paseo Manuel de Lardizabal 4, 20018 Donostia-San Sebastián, Spain

§Escuela de Física, Universidad Nacional de Colombia, Sede Medellín, A. A. 3840, Medellín, Colombia

¶Corresponding author: rita@iff.csic.es

interactions seems to cause minor distortions with the CO_2 guest neighbors interactions do not extending beyond the large $5^{12}6^2$ sI cages. Such findings on these clathrate-like model systems are in accord with experimental observations, drawing a direct relevance to the structural stability of CO_2@sI clathrates.

2 Introduction

Capture and storage/utilization/removal of the CO_2 greenhouse gas is of outstanding importance and a major challenge for gas-control technologies. [1] Scientist are called to identify the right materials and processes for this purpose, with clathrates presenting an excellent source for the formation of inclusion compounds and, thus of great potential for gas storage. [2, 3, 4] Gas clathrate hydrates are nonstoichiometric solid compounds with a cage structure formed by a hydrogen-bonded water network, where guest molecules get trapped. [2] Investigations on clathrate hydrates are largely motivated by the growing need for new energy sources, such as methane and hydrogen clathrates, [5, 6, 7, 8, 9, 10] while more recently mixed-binary clathrates, combining CO_2 and CH_4 as guest gases, have also generated tremendous interest, as possible byproduct storage media and new fuel sources. [7, 11, 12]

CO_2 clathrate hydrates have been mainly found in the sI crystal structure, although some evidence of the CO_2@sII type, and so far binary CO_2@sH clathrates have also been reported. [2, 13, 14, 15, 16, 17, 18] The stability of these clathrates relies on the nature of the guest molecule/s and its interactions with the hydrogen-bonded water network. Commonly, when considering properties of gas clathrate hydrates, semiempirical models are used, as are easier to handle, with a microscopic understanding of the underlying guest-host interactions as well as their effect on macroscopic properties being still far from complete. [19, 20, 21, 22, 23] Nowadays, quantum chemistry approaches, such as wavefunction-based (WF) and density functional theory (DFT) methods could describe such nonstandard guest-host molecular interactions in a reliable way. New methodologies to reduce the computational cost with respect the size of the system aiming to reach linear scaling have been also reported. [24, 25, 26, 27, 28] Therefore, modern first-principles approaches offer the means to explore the molecular interactions of such systems in order to improve our understanding of different physico-chemical processes. [29] Such computational approaches should describe accurately both the hydrogen-bond and dispersion interactions present in gas hydrates, and recent significant improvements have been reported in the performance of dispersion-corrected DFT approximations. [30, 31, 32, 33, 34, 35, 36]

In this work, through reliable electronic DF-MP2 and DFT/DFT-D calculations for isolated finite-size clathrate-like clusters the structural stability of the CO_2@sI cages is investigated. We evaluate the guest-host and inter-cages (cage-cage and guest-guest) effects for the individual building block cages D (small or 5^{12}) and T (large or $5^{12}6^2$) of the CO_2@sI clathrate, as well as two-adjacent aperiodic DT and TT cages, from a bottom-up approach. The im-

pact of the DF-MP2 and different DFT/DFT-D approaches on the interaction and binding of such clathrate-like systems is checked. Due to the restrictions imposed by the highly computational resources demanding as the system size increases, valuable information can be gained from quantum WF-based computations on clathrate-like finite-size systems, [27, 26] where high-accurate *ab initio* WF-based calculations are limited nowadays. [37, 38, 39, 40, 41] Current challenges for investigating the entire periodic clathrate hydrate unit cells via reliable DFT-D, or MP2 approaches [42] are under development, for going beyond system-size scaling and computational performance, although the accuracy of the treatment is still the absolutely key for reliable modeling of hydrate phenomena. Thus, a systematic evaluation of important aspects of the underlying interactions, such as cooperative guest-host and guest-guest/cage-cage effects should be performed.

In this vein, earlier experimental studies have demonstrated [43, 44, 45] that the enclathrated CO_2 molecules show preferred orientations in the sI cages. It has been found that they are rotating rapidly in the large ($5^{12}6^2$ or T) cages, while such rotational motion is suppressed in the dodecahedral (5^{12} or D) cages. Such preferred orientations of the enclathrated CO_2 has been previously reported using different approaches, with not entirely clear results. Recently, the interaction of the CO_2 molecule in isolated sI, sII and sH clathrate cages has been systematically investigated through various DFT approaches, [26] while studies have been also reported on the orientation of the CO_2 in the sI cages or hydrate unit cells using specific DFT approaches. [46, 47, 48] It has been found [26] that the B3LYP functional [49] including the D3M(BJ) correction [32] yields the best performance for all individual CO_2 clathrate cages studied. Also by analyzing [26] the orientation of the CO_2 molecule inside the cages, it has been shown that it depends on the size and symmetry of the cages. So far, for the $CO_2@5^{12}6^2$ sI clathrate cages it has been concluded that the CO_2 is lying on the equatorial plane owing to its oblate shape, as well as in case of the $CO_2@5^{12}6^8$ sH cages, whereas for all other sI, sII and sH cages studied, no such orientational preference is found. This orientation implies rotational ability of the CO_2 in these cages that may play a decisive role in enhancing the stability of the sI and sH crystalline frameworks. Further, in an earlier study it has been reported [22] that by including nuclear quantum effects for the CO_2@sI cages, the rotational ability of the CO_2 is hindered in the D cage, whereas in the T one the translational and rotational degrees of freedom are highly coupled. Such finding has been obtained [22] from quantum approaches employing a semiempirical potential, which shows substantial differences with respect to the benchmark interactions. [26] We should note that anharmonicity could also be crucial to describe the clathrates stability, although they should be explored taking into account realistic underlying interactions. Therefore, it is of particular relevance to access the performance of different generalized-gradient (GGA) and hybrid exchange-correlation functionals, such as revPBE, PW86PBE, and B3LYP, for larger finite-size clusters, like the two-adjacent cage systems considering the effect of first-neighbors inter-cage couplings, for evaluating systematically higher-order guest-host as well as guest-guest and cage-cage

effects. For a direct comparison between data from such clusters calculations, the long-range dispersion corrections were taken into account using different approaches, such as the exchange dipole moment (XDM) model, [50] and the D2/D3/D4 correction schemes. [32]

In this work we attempt to connect the molecular-scale interaction in sI clathrate with a CO_2 guest molecule, and link its microscopic properties to macroscopic observables such as the clathrate's structural stability. We examine the orientation of the confined CO_2 molecule in the sI cages, taking into account the rigidity of all considered cages and their effects on the structure and binding of the clathrate cage/s are determined. CO_2 is a linear molecule with large quadrupole moment that interacts with water molecules through polarizable and dispersion forces. Thus, such finite-size cluster cavities allow to evaluate the role of electrostatic and dispersion interactions from both WF-based and DFT-based computations following a bottom-up approach, starting with the one- and two-cage building-block sI units. The outcome of this study could serve as guideline to further molecular dynamics investigations on such hydrates, contributing to build up improved transferable models able to represent nonstandard noncolavent interactions from nanoclusters up to condensed systems.

Computational details and methods are presented next. Microscopic structure, guest-host and guest-guest/cage-cage energetics in the CO_2@sI cages and the role of the CO_2 molecules orientation on the stability of the clathrate are discussed afterwards. This article ends with a summary and conclusions.

3 Computational setup

CO_2 has been mainly found to form sI type clathrate hydrates. The sI host lattice contains six individual tetrakaidekahedral ($5^{12}6^2$ or T) cages, which are arranged to form two interstitial dodecahedral (5^{12} or D) cages (see lower-left panel in Fig. 1). A non redundant arrangement of such cages is presented in the top panel of Fig. 1, while combinations between D and T adjacent cages are depicted in the lower-right panels. Such two-adjacent cage systems were selected to study the structural stability in terms of first-neighbor effects, through the evaluation of the guest-water, water-water and guest-guest interactions. The two-adjacent cages correspond to the large-small (namely DT) cages with 39 water molecules, large-large (namely TT(5)) cages with 43 water molecules sharing a pentagonal face and large-large (namely TT(6)) cages with 42 water molecules sharing a hexagonal face (see the lower-right panels of Fig.1), and all of them are considered here. Geometry configurations of each individual and two-adjacent cage systems were obtained from the 3D crystalline framework [51] by carving out the crystal sI structure with the DENEB software package [52]. The positions of the oxygen atoms for all water molecules have been determined from the X-ray diffraction experiments, while water proton coordinates in the sI unit cell structure have been chosen to satisfy the ice rules, and by analyzing the symmetry of protons on the hexagonal or pentagonal faces in the hydrate cages

to have the lowest potential energy configuration for the protons, with a net zero dipole moment. Such different proton distributions have been found [51] to show a fairly narrow potential energy spreads, and thus a rather small perturbative effect on the energies of the guests in the cage systems. Thus, in Fig. 1 we display the specific set of proton configurations used in the present computations.

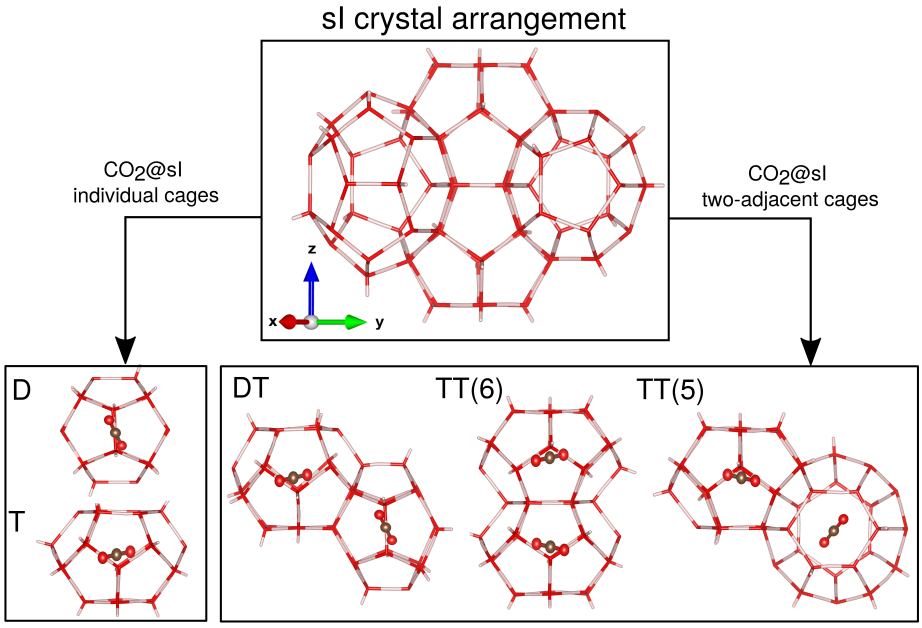

Figure 1: (Upper panel) The sI hydrate crystal cages arrangement. (Lower-left panel) The $CO_2@5^{12}$ and $CO_2@5^{12}6^2$ sI individual clathrate-like cages, namely D and T, respectively. (Lower-right panel) Two-adjacent DT, TT(6) and TT(5) fully occupied CO_2@sI clathrate-like cages (see text). The red color corresponds to the oxygen atoms, the gray to hydrogens, while the brown to carbons.

Electronic structure DFT calculations were performed for the aperiodic clusters of the isolated individual (D and T) and the two-adjacent jointed (DT, TT(6) and TT(5)) cages of the CO_2@sI clathrate hydrate, using the Quantum Espresso (QE) code, [53, 54] while Molpro package [55] was employed for the WF-based computations. Considering the computational cost as the size of the clusters increases, DF-MP2 calculations [55] were carried out using the aug-cc-pVXZ (AVXZ, X=D, T and Q) [56] series of basis sets. The counterpoise corrections (CP), [57] E_{CP}, were included to reduce the basis set superposition error (BSSE) effects in the interaction energies. In turn, all DFT calculations for the isolated cage/s were performed at the Γ-point only, in a cubic simulation cell of volume 30×30×30 Å^3. The Makov-Payne method of electrostatic interaction

correction was considered for these aperiodic systems, where the convergence of the energy is determined by the longest-ranged forces, which usually are electrostatic interactions, evaluated in the limit of large supercells. [58] Full and partial geometry optimizations were performed by relaxing all atomic positions or only those of the CO_2 keeping fixed the water cages, respectively. The BFGS quasi-newton algorithm was employed until components of forces are smaller than 0.05 eV/Å. We used the standard implementation in the LIBXC library [59] for different exchange-correlation functionals, such as the revPBE, PW86PBE, and B3LYP, together with a variety of their dispersion-corrected analogs by means of various semi-classical density based corrections. We choose to employ the B3LYP functional, as in a previous study on different CO_2 clathrate's cages it has been shown to best-perform compared to benchmark data, [26] although for larger clusters it became computationally demanding, especially in the geometry optimization calculations involved. So, bearing in mind to deal with large number of molecules noncovalent systems alternatives, such as the revPBE and PW86PBE functionals, as implemented in QE code, [53, 54] were also considered. Regarding the dispersion correction schemes a variety of them were employed, such as the semiempirical D2, [60] the original zero-damping function D3(0), [61] the most popular Becke-Johnson damping function D3(BJ), [62] the D3M(0) [63] and the D3M(BJ), [63] using the DFTD3 program, [64] while the DFTD4 code [65] was used to count for the corrections from the most recent developed D4 [66, 67] model including many-body dispersion interactions beyond the pairwise terms. The XDM model, like the D3 scheme, contains three-body intermolecular dispersion contributions and was also considered here, using the POSTG code [68] with its damping function parameters a_1 and a_2(Å) parameterized for different functionals. [50]

Interaction and binding energies are calculated as the difference of the total energy of the fully or partial occupied CO_2@sI cage/s systems, and the energies of the empty cage/s and the n CO_2 molecules (being in total maximum of two/one per cage) given by

$$\Delta E_{int} = E_{CO_2@sI\,cage} - E_{sI\,cage} - n.E_{CO_2} \quad \text{and} \tag{1}$$

$$\Delta E = E^{opt}_{CO_2@sI\,cage} - E^{opt}_{sI\,cage} - n.E^{opt}_{CO_2}, \tag{2}$$

at any selected and geometry-optimized (full or partial) configurations, respectively. We should emphasize that binding energies are a particular instance of interaction energies at the optimized configurations of the systems under study. The cohesive energies for each N water cage (empty) system are obtained as the difference of the cluster energy and the energies of the geometry-relaxed water monomers, $\Delta E_{coh} = E_{(sIcage)_N=20,24,39,42,43} - N.E_{H_2O}$. Comparisons of such binding energies enable to account for the guest-water/guest-guest/water-water strength on the stability of the clathrate-like clusters. Further, comparisons of the optimized geometries provide information on preferential occupation and structural orientation preference of the CO_2 in each sI cage/s under study.

4 Results and Discussion

4.1 Assessing DFT-derived interactions

As mentioned, recent benchmark DF-MP2/CBS and DFT calculations have been reported [26] for all individual sI, sII and sH cages of the CO_2 hydrates, and it has been shown that the B3LYP-D3M(BJ) approach offers a reliable description of the guest-host interactions. In the same vein, the effects of guest-cage as well as the inter-cages interactions could be further explored from a bottom-up approach, if the same DFT computations are performed for larger-size, although computationally manageable, systems, such as those consisting of individual sI cages or two-adjacent sI cages, where in the latter systems one can also evaluate the influence of the nearest neighbors on the interactions.

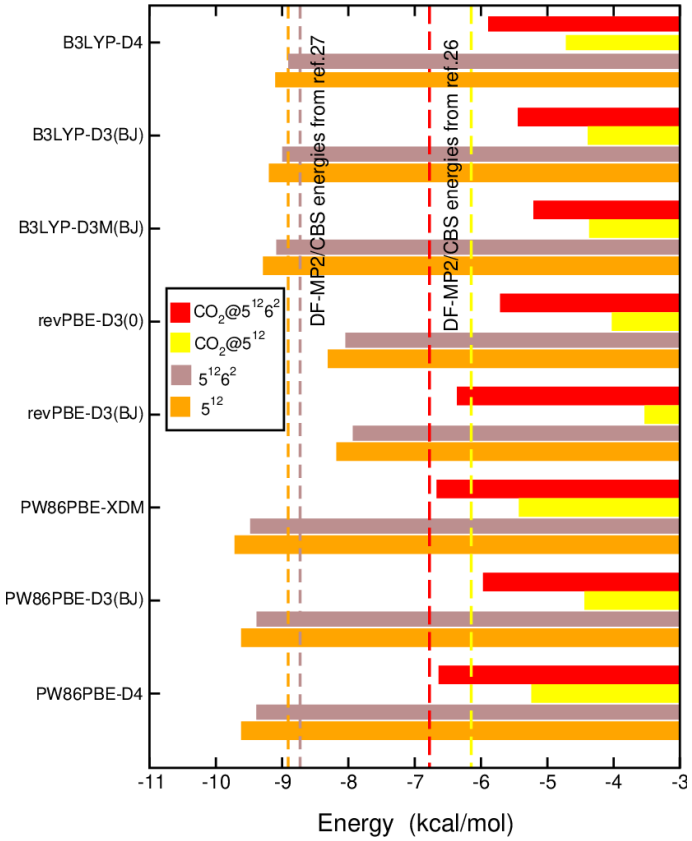

Figure 2: Interaction and cohesive (per water molecule) energies of the individual CO_2-filled and empty 5^{12} (or D) and $5^{12}6^2$ (or T) sI cages, respectively, obtained from the indicated DFT-D calculations. Vertical long-dashed and dashed lines correspond to the DF-MP2/CBS[TQ] and DF-MP2/CBS[Q5] energies from refs. [26, 27], respectively.

Thus, we first considered the D and T individual sI cages (see lower-left panel in Fig. 1) in a cubic supercell, and we explored interaction energies and cohesive energies of the CO_2-filled and empty sI cages, respectively. In Fig. 2 we display the interaction energies obtained using the indicated revPBE, PW86PBE and B3LYP DFT/DFT-D functionals, that were found to perform best in estimating the binding energies of the $CO_2@5^{12}$ and $CO_2@5^{12}6^2$, together with cohesive energies of the empty T and D cages (see Table S1 in supporting information). The reference DF-MP2/CBS energies for both CO_2-filled and empty D and T individual sI cages are also displayed [26, 27] (see vertical dashed and long-dashed lines in Fig. 2, respectively). By comparing the DFT-D functionals with the reference data available in the literature from WF-based methods, we should note that the examined D3 variants, the D4 and XDM schemes yield similar energy values for each functional, with the PW86PBE-XDM and PW86PBE-D4 estimates being closer to the DF-MP2/CBS data for both filled and empty T and D cages. The B3LYP with D3(BJ), D3M(BJ) and D4 corrections underestimates the interaction of the CO_2 with both cages, while yields cohesive energies for the empty sI cages in very good accord with the reference values. The revPBE-D3(0) and revPBE-D3(BJ) results are found to underestimate both interaction and cohesive energies for the D and T sI cages. All functionals under study predict that the interaction energies are larger for the T cage than the D one, indicating that $CO_2@5^{12}6^2$ configurations are more stable than the $CO_2@5^{12}$, in accord with previous studies. [69, 47, 48, 26]

In turn, we also examined the structures corresponding to the two-adjacent DT, TT(6) and TT(5) sI cages (see lower-right panel in Fig. 1) of 39, 42 and 43 water molecules, respectively. In particular, we computed both DF-MP2/AVTZ (including CP corrections) and DFT-D interaction energies for all these (both fully and partially CO_2 occupied) cage systems employing the same functionals as in the individual D and T cages: the B3LYP including the D3(BJ) and D4, the PW86PBE with the XDM, D3(BJ) and D4 dispersion corrections, and the revPBE, with the D3(0) and D3(BJ) schemes. For the DT cages, we considered the fully occupied (1+1), the (1+0) occupying only the D cage, and the (0+1) when only the T cage is occupied, configurations, while in the TT(5) and TT(6) cases, the fully occupied (1+1), as well as the (1+0) and (0+1) configurations, when only one of the T cages is occupied, were considered.

In Fig. 3 we show the interaction energies for the DT, TT(5) and TT(6) systems considering the CO_2 configurations previously described. The dashed lines indicate the DF-MP2/AVTZ reference data for each of these systems (see Table S2 in supporting information). The PW86PBE functional with XDM and D4 dispersion corrections was found to provide estimates with energy difference values less than 0.6 and 0.7 kcal/mol, respectively, compared to the reference DF-MP2/AVTZ data, while the revPBE-D3(0)/D3(BJ) and B3LYP-D3(BJ)/D3M(BJ)/D4 underestimate the interaction energies for all nine different DT, TT(5) and TT(6) systems with differences up to 2.4 kcal/mol (see Table S2 in supporting information).

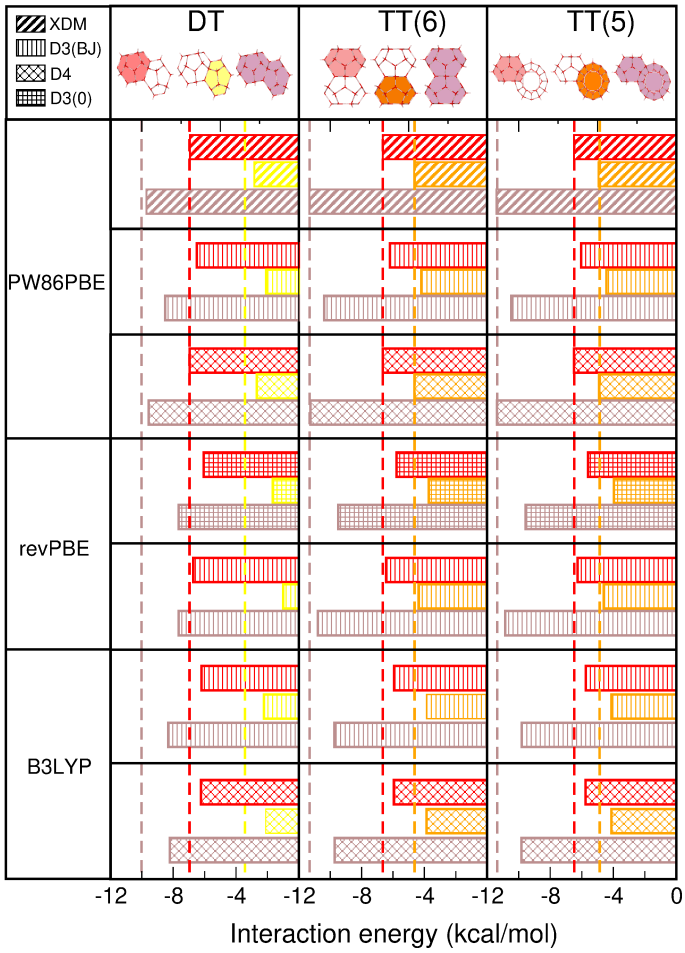

Figure 3: Interaction energies for the full (1+1) and partial (1+0)/(0+1) CO_2-occupied DT, TT(5), TT(6) adjacent sI cages, obtained from the indicated DFT-D calculations. Reference DF-MP2/AVTZ values are plotted by vertical color dashed lines as indicated for each case.

As it was expected, we found that dispersion has a strong effect on the energies, and reliable results obtained when dispersion effects are treated properly. Although different functionals employed here, show variations in the interaction energy values, when dispersion corrections are added, then the trends were found to be similar for all CO_2@sI cage systems studied here (see Table S1 in the supporting information). Interestingly, comparison of the DF-MP2 and DFT-D energies shows similar behavior for all individual and two-adjacent sI cages considered (see Figs. 2 and 3). It was found that, the CO_2 interacts more strongly with the larger T cages than the D ones. As expected the guest-host interaction depends on both the cage size and symmetry, as well as the shape

of the guest molecule. In agreement with previous experimental and theoretical studies [44, 70, 45, 22, 26] the orientational preference of the CO_2 in the sI cages permits its rotation, and it may enhance the stability of the CO_2@sI clathrates. As inter-cage interactions should also expected to contribute, so such guest-guest and cage-cage effects are analyzed in following section by studying the energetics and structuring for the progressive CO_2 occupation of the sI cage systems.

4.2 Energetics and structural stability: the role of CO_2 orientation

Once we check the performance of various electronic structure methods in the following we proceed geometry relaxation calculations to evaluate the structural stability of the sI clathrate-like cages under study. We have carried out optimization employing the PW86PBE-XDM functional considering both rigid and flexible cage/s. Previous studies have supported [71, 22, 69, 8, 48, 26] single occupancy of the CO_2@sI clathrate cages, so optimizations for each sI cage/s containing one CO_2 per cage were considered.

We have first optimized the empty cage/s, and in turn we reoptimized the CO_2 inclusion complexes. We also checked the cage rigidity for all the CO_2 filled (partial/full) cage/s, by carrying out partial optimizations keeping fixed the corresponding sI cage/s. In this way the binding energies with respect to the guest-free system are calculated, and at the same time the effect of the CO_2 enclathration in the cage shape is evaluated. The corresponding results of such computations are given in Table S3 in the supporting information. All such progressive (single) occupation processes are shown in Fig. 4 for the D and T, as well as all combinations of the DT, TT(5) and TT(6) two-adjacent sI cages, with binding energies displayed for each of the steps. Binding energies are computed for both rigid and relaxed sI cages. The values in bold indicate the binding energy for fully occupied sI cages, while those in black correspond to partial cages filling. Also, we should note that the stability for the CO_2 inclusion complexes calculated by the full optimized sI cages is very comparable with the values obtained from the partial geometry optimizations with the CO_2 molecules inside the rigid sI cages. Such finding indicates the rigidity of the water cages arrangement, although some water molecules that participated in guest-host bonding were reoriented, nevertheless, the original water-water hydrogen bonds were preserved, with some exception in the outer hydrogen atoms orientation.

For all clathrate-like cage systems studied, it is clear that there is a significant preference of CO_2 for occupying the T cage, in agreement with previous studies. [22, 47, 8, 48, 26] According to the present computations the energy difference between the individual D and T sI cages is about 1.7 kcal/mol, while in the case of the two-adjacent cage systems the most energetically efficient filling process is when CO_2 molecules occupy the TT(5) cages with energy of -12.5 kcal/mol, although similar values of -12.2 and -11.4 kcal/mol are obtained for the fully filled DT and TT(6) two-adjacent cages, respectively. The interaction energy of the CO_2 increases as the size of the individual cage increases, and

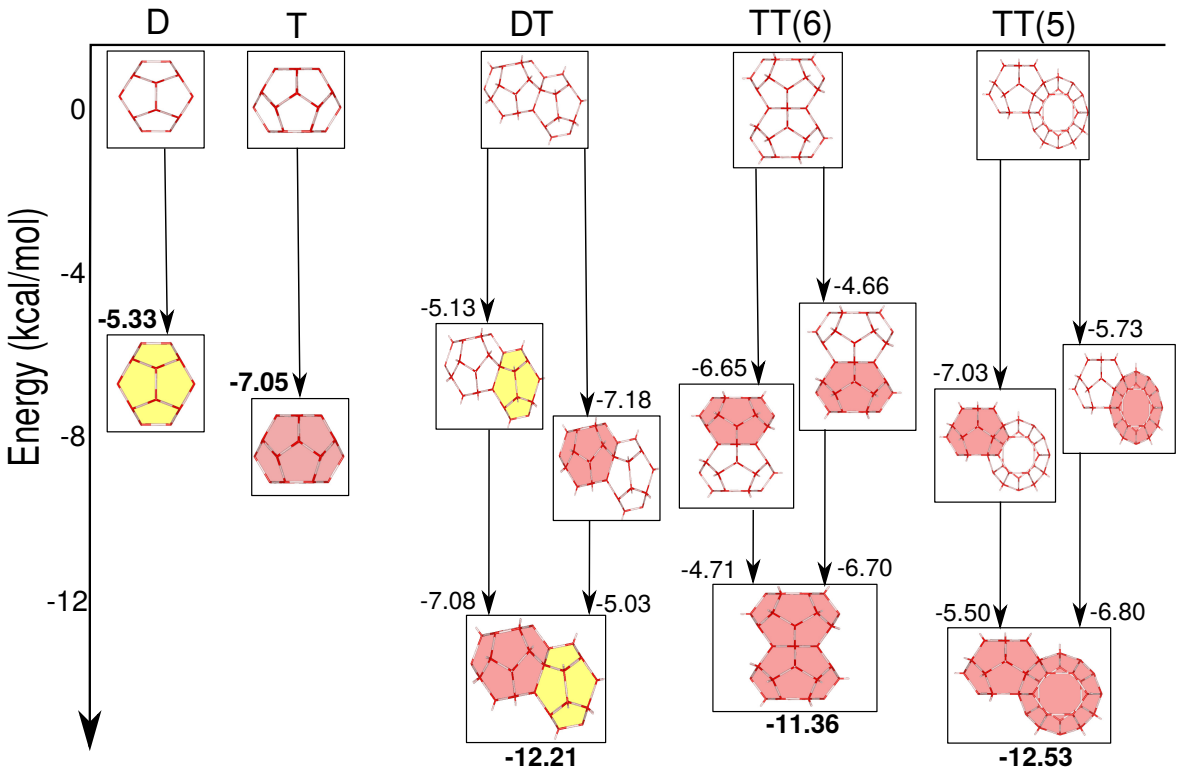

Figure 4: Binding energy (in kcal/mol) for the D, T, DT, TT(6) and TT(5) sI (rigid) cages, formed by 20, 24, 39, 42 and 43 water molecules for gradual CO_2 occupation.

among the cases studied, its interaction with the DT is more attractive counting -7.18 kcal/mol. In all two-adjacent sI cages a CO_2-cage pairwise interaction approach predicts more stable configurations than those computed, indicating that higher-order many-body effects destabilize them, especially the TT(6) and TT(5) ones, except in the (0+1) CO_2@DT case. Also, one should expect that in the TT(5) and TT(6) cases the interaction energies of partial occupation should be closer, although the presence of the neighboring empty cage clearly affects the energetics. By analyzing the interaction and binding energy values obtained for fixed CO_2 orientations for the partial (1+0) and (0+1) with those found from geometry optimizations in the individual rigid D and T sI cages, one could evaluate the effect on the energy by the presence of the neighbors (see Tables S1, S2 in the supporting information and Fig. 4). In the case of the TT(6) system we observed the smaller differences, while in the DT are the larger when the CO_2 occupies the D cage. The multipolar interactions between CO_2 and the host (water) cage/s result in stronger guest-host forces, and apart of the size of the cage also the shape of the guest molecule contributes to such

relatively high energy values. The resulting directional attractive interactions can be attributed to the linear shape of the CO_2 as it interacts only with a limited number of the surrounding water molecules of the sI cage/s. Thus, the influence on the guests' orientation by the presence of the neighbor cages will be discussed next.

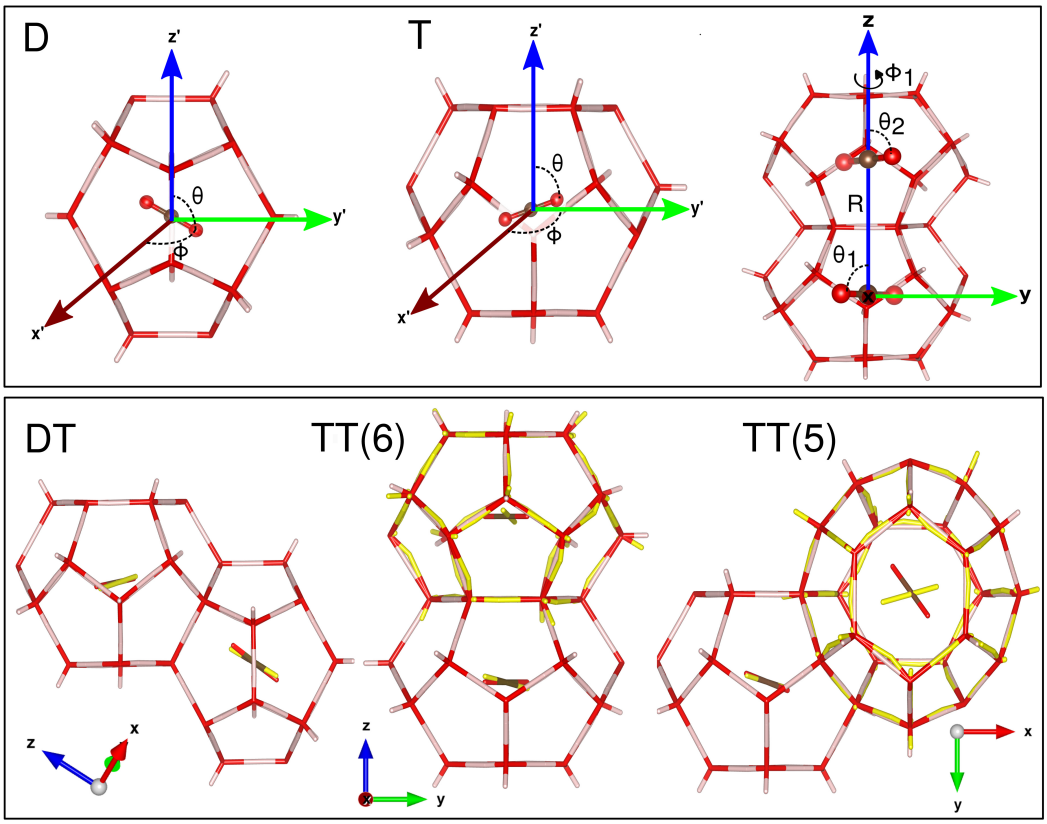

Figure 5: Orientation of CO_2 molecules inside the individual D and T, as well as in the full (1+1) occupied DT, TT(6) and TT(5) two-adjacent sI cages. The coordinate systems used in both individual and two-adjacent sI cages are also displayed. For the encapsulated CO_2 molecules their orientations in the individual D and T sI cages are also shown with yellow color for the oxygen atoms, and brown for carbons, while also for comparison reasons with yellow color the individual T cage is superimposed when differences are obtained (see text).

The orientation of the single CO_2 molecule in each sI cage is shown in Figure 5, and we found that its inclusion is energetically favorable. We should

emphasize that the D cage is formed by twelve pentagons, while the T cage is anisotropic, consisting of two six-membered and twelve five-membered rings. A comparison of the progressive occupied optimized systems shows that orientational preference varies among them. Starting with the individual D and T cages (see upper-left panel of Figure 5), the results on the CO_2 orientation from the partial optimizations are found in accord with those previous reported. [44, 45, 22, 26] In particular, for the D cage CO_2 is located at the center of the cage with θ=60 ° and ϕ=90 ° (see corresponding coordinate system at the upper-left panel of Figure 5), while for the T cage values of θ=100 ° and ϕ=45 ° (see corresponding coordinate system at the upper-middle panel of Figure 5) were obtained with the CO_2 shifted from the cage's center by 0.08 Å. Almost the same values are obtained from the full optimizations for the CO_2@T cage, while slight differences were found for the CO_2@D cage, with θ=56 ° and ϕ=94 °. However, one should be aware of the influence of the limited size of the individual cage model, as in actual clathrates each water molecule participates in four hydrogen bonds, and thus its reorientation would be most probably limited in comparison with the present full optimized case, and guest-host effects should be described better in the case of the individual rigid cages results.

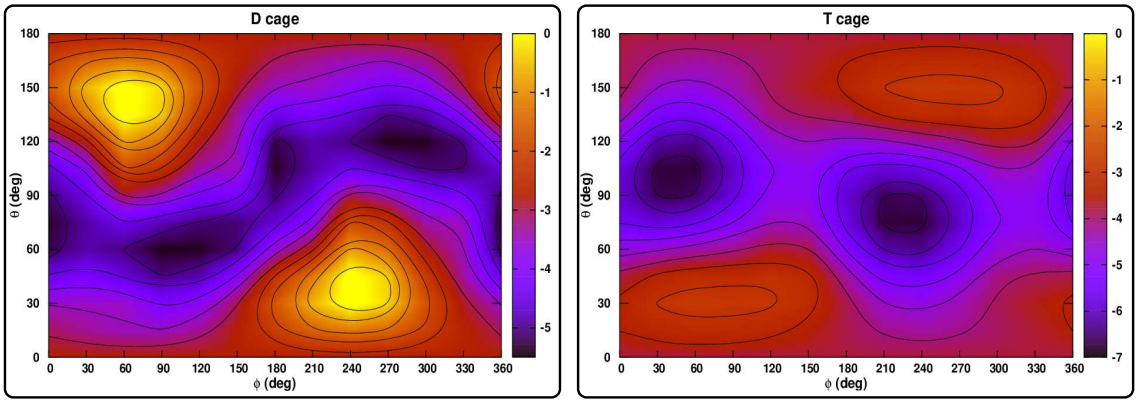

Figure 6: Contour plots of the potential energy in the (ϕ,θ)-plane of the CO_2 molecule inside the individual rigid D (left panel) and T (right panel) cages. The equipotentials are plotted from -5.5 to -0.5 kcal/mol and -7.0 to -2.5 kcal/mol for the D and T cases, respectively, with intervals of 0.5 kcal/mol.

Apart to the specific preference of the CO_2 orientation, in Fig. 6 we display contour plots of how the potential varies as a function of θ and ϕ angles (see coordinate system in upper panel of Fig. 5) in each of the rigid D (left panel) and T (right panel) cages. The dark blue color equipotentials correspond to the minima energy values, while red and yellow color regions to higher energy ones. One can see that in the T cage for θ angles around the equatorial plane at 90°, between 70 and 110°, the CO_2 can freely rotate in ϕ, while in the D cage such rotation of the guest molecule is pretty much hindered with high potential

barriers nearby. These findings are in agreement with previous experimental observations in diffraction measurements [44, 45], with such preference orientation and rotational ability of the CO_2 in T cages contributing to the the stability of the CO_2@sI clathrates.

Another important contribution is expected from the guest-guest and cage-cage interactions, so we aim to get such information by exploring the two-adjacent cages model. In Fig. 5 (see lower panels) we display the orientation of the CO_2 molecules in the fully occupied (1+1) cases using the (r, θ, ϕ) and (R, θ_1, θ_2, ϕ_1) coordinates, as shown in the upper panels of the figure, with respect the individual and two-adjacent sI cages, respectively, whereas the results from the partial (1+0) and (0+1) occupations are given in Table S4 in the supporting information. For the purpose of comparison, we also superimposed in yellow color the orientation of the CO_2 with respect to the (r, θ, ϕ) coordinate system for each of the individual D and T cages. Recall that both individual and two-adjacent cage systems are part of the same sI crystal, and one of the T cages is common in all two-adjacent systems studied. In general, one can see how the CO_2 maintains its orientations as those in the individual D and T cages, with larger variations due to different outer hydrogen orientations in one of the T cage (see upper and right T cages in the TT(6) and TT(5), respectively). This trend is also observed for the progressive CO_2 occupation in the (1+0) and (0+1) configurations. Our results from the partial optimizations are in close accord with previous reported data from experimental observations. [43, 44, 45] In the case of the full geometry optimizations (see Table S4 in the supporting information), again, no significant differences are observed for the CO_2 orientation in the T cages, however inside the D cage it highly depends of the rigidity of the DT cage system. In particular, the orientation of the CO_2 in the D cage from partial and full geometry optimizations, shows differences in θ and ϕ angles in both (1+0) and (1+1) cage systems. For the fully occupied (1+1) rigid DT, TT(6) and TT(5) systems the relative configurations of the two CO_2 molecules are R= 6.98, 6.05 and 7.36 Å, θ_1= 7, 90, and 109 °, θ_2=54, 90 and 104 °, and ϕ_1=52, 90, and 69 °, respectively. One can see that the intermolecular R distance between the two CO_2 molecules in the adjacent sI cages , as well as their relative orientations in the TT(6) and TT(5) systems are quite different, indicating the influence of the water molecules in the intermediate hexagonal and pentagonal faces of the two-adjacent sI cages. The shorter R distance is obtained in the TT(6) cages, while the longer in the TT(5) ones. Further, by comparing with the isolated CO_2-CO_2 interactions [72] at the asymptotic region, one can conclude that the orientation of the two CO_2 is clearly marked by their interaction with the surrounding water framework, while the guest-guest interaction between them, especially in the CO_2@TT(5) case, does not extend beyond the T cages. This can be also seen by the differences observed in the CO_2 orientations between the (1+0) and (0+1) configurations of the CO_2@TT(5) and CO_2@TT(6) systems, from both full and partial optimizations, mainly in ϕ angle. Such deviations are also present in the (1+1) CO_2@TT(5) and CO_2@TT(6) cages, and are attributed to the slight distortion of one of the T cages in the two-adjacent sI cages systems, as it shown in yellow color in Fig. 5, compared

to the individual T one, with the outer hydrogen reorientation affecting mainly the ϕ angle values. In contrary, in the CO_2@DT case, the cage-cage effects are important as they affect the CO_2 orientation in the D cage with ϕ being around 70° in the (1+0) compared with ϕ=90° in the individual CO_2@D cage, while guest-guest interactions influence just slightly the CO_2 orientation, with ϕ=75°, in the (1+1) CO_2@DT rigid cage system. In other words, by carrying out full optimization calculations, we conclude that the cage-cage interactions don't affect the structural stability of the CO_2@TT(6) and CO_2@TT(5) systems, while in the CO_2@DT case such interactions contribute to slightly reorientate the CO_2 only in the small D cage by increasing the stability of the (1+1) CO_2@DT model system. However, we should point out that comparisons of the present findings with experimental observations confirm the rigidity of the CO_2@sI cages, with exception in the orientation of the outer hydrogens in all cluster models studied.

5 Summary and conclusions

By combining modern quantum chemistry technologies new information is provided regarding the underlying potential energy interactions, and structural stability of CO_2 molecules inside cages of sI clathrate hydrates.

First-principles DFT-D calculations have been carried out by considering GGA and hybrid functionals, and interaction energies are compared to *ab initio* data obtained from well-converged DF-MP2 computations, for both individual and two-adjacent cages of the CO_2@sI clathrate hydrates. It has been found that the selected DFT functionals show similar trends, and the PW86PBE functional with XDM or D4 corrections is considered to best-perform, providing reliable energetics for both individual and two-adjacent CO_2@sI clathrate cages. The role of the dispersion forces is investigated, and it has been shown their strong effect on the interaction energies of all CO_2 clathrate-like systems under study.

Geometry relaxations (full and partial) have been performed yielding the DFT-derived structural and stability properties of such clathrate-like systems. Thus, their structural stability, by balancing guest-water, guest-guest and water-water interactions, is discussed, and the impact of progressive cage occupancy with a single guest CO_2 molecule is evaluated. The single CO_2 occupancy of the individual T sI cage was found to be energetically more favorable than that of the D sI cage, and such preference is attributed to the influence of the guest molecule shape/size on the guest-water interactions. The same effect is also observed when considering the binding energies of the full and partial occupied two-adjacent sI cage systems, where first-neighbors guest-guest and water-water interactions are present. The fully CO_2 occupied TT(5) cage system is found to be more stable than the DT and TT(6) ones, although their binding energies are within 0.3 and 1.2 kcal/mol, respectively. The current computational study clearly reveals that the individual D and T sI water cages as well as in the two-adjacent DT sI cages remain almost intact upon the CO_2 capture, while in the cases of the two-adjacent TT(5) and TT(6) cage systems, one of the T cages shows some distortion mainly in the orientation of the outer hydrogen

atoms, and addresses the role played by the preferential orientation of the CO_2 molecule/s on the stabilization of different cages.

Understanding such structural preference requires a detailed investigation of the underlying molecular interactions. The present results of such bottom-up approach corroborate very well with the observation that CO_2 enclathration is dominating by guest-size and shape effects. The stability was analyzed by considering the optimal orientation of the enclathrated CO_2 molecule/s, taking into account the guest-host and inter-cages (guest-guest and water-water) couplings. Such interactions play a significant role in the structure, stability, and properties of these compounds, and their understanding is a key to control the structure-property relations for the different technological applications. Thus, it would be extremely interesting to provide additional insights on the underlying factors governing such structural preference considering the crystal environment. Such complementary information is still needed, and we expect that the current study will trigger new theoretical and experimental efforts in this direction, leading in developing improved predictive models. In this context, many-body potentials are ultimately necessary to achieve the goal of describing macroscopic properties from a rigorous microscopic view. Data from such bottom-up approaches combined with truncated many-body expansion representations [41, 10], beyond traditional pairwise terms, present a promise and rational route to follow to model large systems in a systematic way. This requires further information on the molecular interactions for ascertaining the importance of higher-order effects, and investigations on the stability of different structure type CO_2 clathrate hydrates, such as sII and sH, as well as their multiple CO_2 cage occupancy should be also considered. On this basis the outcome of this work aims to guide such future DFT investigations for the entire periodic crystalline network, in order to fine-tune errors and deficiencies for controlling the stabilization of these promising CO_2 storage materials.

6 Acknowledgement

We would like to thank Raúl Rodríguez-Segundo and José A. Torres for useful discussions on DENEB software. The authors thank to Centro de Cálculo del IFF, SGAI (CSIC) and CESGA for allocation of computer time. This work has been supported by MINECO grant No. FIS2017-83157-P, Comunidad de Madrid grant No. IND2017-AMB7696, "CSIC for Development" (i-COOP) grant ref: ICOOPB20214, Hermes code: 49572 (Universidad Nacional de Colombia) and COST Action CA18212(MD-GAS).

7 Keywords

clathrate-like clusters, CO_2 hydrates, electronic structure calculations, guest-host interactions

8 TOC

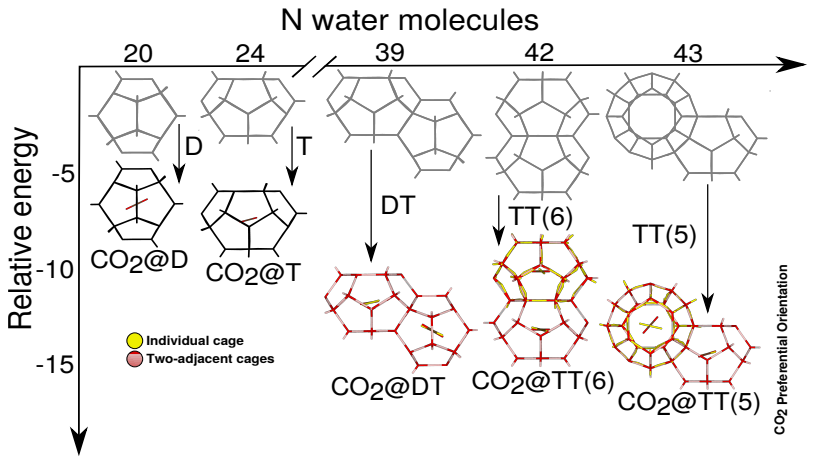

Relative structural stability of the CO_2@sI hydrates: guest-cage interactions and inter-cage couplings in clathrate-like systems.

References

[1] M. Goel, M. Sudhakar, R.V. Shahi, *Carbon Capture, Storage and Utilization - A Possible Climate Change Solution for Energy Industry*. CRC Press, **2019**.

[2] E. D. Sloan, C. A. Koh, *Clathrate Hydrates of Natural Gasess*. CRC Press, 3rd edition edition, **2007**.

[3] C. A. Koh, E. D. Sloan, *AIChE J.* **2009**, *53*, 1636–1643.

[4] C. A. Koh., E. D., A. K. Sum, D. T. Wu, *Annu. Rev. Chem. Biomol. Eng.* **2011**, *2*, 237–257.

[5] V. V. Struzhkin, B. Militzer, W. L. Mao, H. K. Mao, R. J. Hemley, *Chem. Rev.* **2007**, *107*, 4133–4151.

[6] S. Y. Willow, S. S. Xantheas, *Chem. Phys. Lett.* **2012**, *525*, 13–18.

[7] Z. R. Chong, S. H. B. Yang, P. Babu, P. Linga, X. S. Li, *Appl. Energ.* **2016**, *162*, 1633–1652.

[8] J. Jia, Y. Liang, T. Tsuji, S. Murata, T. Matsuoka, *Sci. Rep.*, **2017**, *7*, 1290.

[9] Z. Futera, M. Celli, L. Rosso, C. J. Burnham, L. Ulivi, N. J. English, *J. Phys. Chem. C* **2017**, *121*, 3690–3696.

[10] C. Ou, J. M. Bowman, *J. Phys. Chem. A* **2018**, *123*, 329–335.

[11] R. Boswell, D. Schoderbek, T. S. Collett, S. Ohtsuki, M. White, B. J. T Anderson, *Energ. Fuel.* **2016**, *31*, 140–153.

[12] A. Striolo, *Mol. Phys.* **2019**, *117*, 3556–3568.

[13] H. Hirai, K. Komatsu, M. Honda, T. Kawamura, Y. Yamamoto, T. Yagi, *J. Chem. Phys.* **2010**, *133*, 124511.

[14] F. Fleyfel, J. P. Devlin, *J. Phys. Chem.* **1991**, *95*, 3811–3815.

[15] D. K. Staykova, W. F. Kuhs, A. N. Salamatin, T. Hansen, *J. Phys. Chem. B* **2003**, *107*, 10299–10311.

[16] T. M. Narayanan, K. Imasato, S. Takeya, S. Alavi, R. Ohmura, *J. Phys. Chem. C* **2015**, *119*, 25738–25746.

[17] Y. Lee, D. Lee, J. W. Lee, Y. Seo, *Appl. Energ.* **2016**, *163*, 51 – 59.

[18] B. R. Cladek, S. M. Everett, M. T. McDonnell, M. G. Tucker, D. J. Keffer, C. J. Rawn, *J. Phys. Chem. C* **2019**, *123*, 26251–26262.

[19] S. Alavi, T. K. Woo, *J. Chem. Phys.* **2007**, *126*, 044703.

[20] A. Vítek, D. J. Arismendi-Arrieta, R. Rodriguez-Cantano, R. Prosmiti, P. Villarreal, R. Kalus, G. Delgado-Barrio, *Phys. Chem. Chem. Phys.* **2015**, *17*, 8792–8801.

[21] J. M. Míguez, M. M. Conde, J. P. Torré, F. J. Blas, M. M. Pineiro, C. Vega, *J. Chem. Phys.* **2015**, *142*, 124505.

[22] A. Valdés, D. J. Arismendi-Arrieta, R. Prosmiti, *J. Phys. Chem. C* **2015**, *119*, 3945–3956.

[23] D. J. Arismendi-Arrieta, A. Vítek, R. Prosmiti, *J. Phys. Chem. C* **2016**, *120*, 26093–26102.

[24] C. Riplinger, P. Pinski, U. Becker, E. F. Valeev, F. Neese, *J. Chem. Phys.* **2016**, *144*, 024109.

[25] A. A. Mostofi, P. D. Haynes, C. K. Skylaris, M. C. Payne, *Mol. Simul.* **2007**, *33*, 551–555.

[26] D. J. Arismendi-Arrieta, A. Valdés, R. Prosmiti, *Chem. Eur. J.* **2018**, *24*, 9353–9363.

[27] I. León-Merino, R. Rodríguez-Segundo, D. J. Arismendi-Arrieta, R. Prosmiti, *J. Phys. Chem. A* **2018**, *122*, 1479–1487.

[28] R. Yanes-Rodríguez, D. J. Arismendi-Arrieta, R. Prosmiti, *J. Chem. Inf. Model.* **2020**, *60*, 3043–3056.

[29] B. C Barnes, A. K Sum. *Curr. Opin. Chem. Eng.* **2013**, *2*, 184–190,

[30] E. R. Johnson, I. D. Mackie, G. A. DiLabio. *J. Phys. Org. Chem.* **2009**, *22*, 1127–1135,

[31] J. Klimeš, A. Michaelides, *J. Chem. Phys.* **2012**, *137*, 120901.

[32] S. Grimme, A. Hansen, J. G. Brandenburg, C. Bannwarth, *Chem. Rev.* **2016**, *116*, 5105.

[33] D.G. A. Smith, L. A. Burns, K. Patkowski, C. D. Sherrill, *J. Phys. Chem. Lett.* **2016**, *7*, 2197–2203.

[34] J. Hermann, R. A. Distasio, A. Tkatchenko, *Chem. Rev.* **2017**, *117*, 4714.

[35] J. Witte, N. Mardirossian, J. B. Neaton, M. Head-Gordon, *J. Chem. Theory Comput.* **2017**, *13*, 2043–2052.

[36] M. G. Medvedev, I. S. Bushmarinov, J. Sun, J. P. Perdew, K. A. Lyssenko, *Science* **2017**, *355*, 49–52.

[37] N. J. English, J. M. D. MacElroy, *Chem. Eng. Sci.* **2015**, *121*, 133–156.

[38] E. Miliordos, S. S. Xantheas, *J. Chem. Phys.* **2015**, *142*, 234303.

[39] M. J. Gillan, D. Alfé, A. Michaelides, *J. Chem. Phys.* **2016**, *144*, 130901.

[40] B. R. L. Galvão, L. P. Viegas, *J. Phys. Chem. A* **2019**, *123*, 10454–10462.

[41] Q. Wang, J. M. Bowman, *J. Chem. Phys.* **2017**, *147*, 161714.

[42] G. J. Beran, *Chem. Rev.* **2016**, *116*, 5567–5613.

[43] T. Ikeda, O. Yamamuro, T. Matsuo, K. Mori, S. Torii, T. Kamiyama, F. Izumi, S. Ikeda, S. Mae, *J. Phys. Chem. Solids* **1999**, *60*, 1527–1529.

[44] K. A. Udachin, C. I. Ratcliffe, J. A. Ripmeester, *J. Phys. Chem. B* **2001**, *105*, 4200–4204.

[45] S. Takeya, K. A. Udachin, I. L. Moudrakovski, R. Susilo, J. A. Ripmeester, *J. Am. Chem. Soc.* **2010**, *132*, 524–531.

[46] A. Vidal-Vidal, M. Pérez-Rodríguez, J. P. Torré, M. M. Piñeiro, *Phys. Chem. Chem. Phys.* **2015**, *17*, 6963–6975.

[47] F. Izquierdo-Ruiz, A. Otero-de-la Roza, J. Contreras-García, O. Prieto-Ballesteros, J. M. Recio, *Materials* **2016**, *9*, 777.

[48] M. Pérez-Rodríguez, A. Vidal-Vidal, J. M. Miguez, F. J. Blas, J.-P. Torré, M. M. Piñeiro, *Phys. Chem. Chem. Phys.* **2017**, *19*, 3384–3393.

[49] A. D. Becke, *J. Chem. Phys.* **1993**, *98*, 5648–5652.

[50] A. D. Becke, E. R. Johnson, *J. Chem. Phys.* **2007**, *127*, 154108.

[51] F. Takeuchi, M. Hiratsuka, R. Ohmura, S. Alavi, A. K. Sum, K. Yasuoka, *J. Chem. Phys.* **2013**, *138*, 124504.

[52] Deneb 1.30 beta: The nanotechnology software by Atelgraphics, **2020**, https://www.atelgraphics.com.

[53] P. Giannozzi, S. Baroni, N. Bonini, M. Calandra, R. Car, C. Cavazzoni, D. Ceresoli, G. L. Chiarotti, M. Cococcioni, I. Dabo, A. Dal Corso, S. de Gironcoli, S. Fabris, G. Fratesi, R. Gebauer, U. Gerstmann, C. Gougoussis, A. Kokalj, M. Lazzeri, L. Martin-Samos, N. Marzari, F. Mauri, R. Mazzarello, S. Paolini, A. Pasquarello, L. Paulatto, C. Sbraccia, S. Scandolo, G. Sclauzero, A. P. Seitsonen, A. Smogunov, P. Umari, R. M. Wentzcovitch, *J. Phys.: Condens. Matter* **2009**, *21*, 395502.

[54] P. Giannozzi, O. Andreussi, T. Brumme, O. Bunau, M. Buongiorno-Nardelli, M. Calandra, R. Car, C. Cavazzoni, D. Ceresoli, M. Cococcioni, N. Colonna, I. Carnimeo, A. Dal Corso, S. de Gironcoli, P. Delugas, R. A. DiStasio Jr, A. Ferretti, A. Floris, G. Fratesi, G. Fugallo, R. Gebauer, U. Gerstmann, F. Giustino, T. Gorni, J. Jia, M. Kawamura, H-Y. Ko, A. Kokalj, E. Küçükbenli, M. Lazzeri, M. Marsili, N. Marzari, F. Mauri, N. L. Nguyen, H-V. Nguyen, A. Otero de la Roza, L. Paulatto, S. Poncé, D. Rocca, R. Sabatini, B. Santra, M. Schlipf, A. P. Seitsonen, A. Smogunov, I. Timrov, T. Thonhauser, P. Umari, N. Vast, X. Wu, S. Baroni, *J. Phys.: Condens. Matter* **2017**, *29*, 465901.

[55] H.J. Werner, P. J. Knowles, G. Knizia, F. R. Manby, M. M. Schütz, and et al., **2012**, http://www.molpro.net.

[56] R. A. Kendall, T. H. Dunning Jr., R. J. Harrison, *J. Chem. Phys.* **1992**, *96*, 6796–6806.

[57] S. F. Boys, F. Bernardi, *Mol. Phys.* **1970**, *19*, 553–566.

[58] G. Makov, M. C. Payne, *Phys. Rev. B* **1995**, *51*, 4014.

[59] M. A.L. Marques, M. J. T. Oliveira, T. Burnus, *Comput. Phys. Commun.* **2012**, *183*, 2272–2281.

[60] S. Grimme, *J. Comput. Chem.* **2006**, *27*, 1787–1799.

[61] E. Grimme, J. Antony, S. Ehrlich, H. Krieg, *J. Chem. Phys.* **2010**, *132*, 154104.

[62] E. Grimme, S. Ehrlich, L. Goerigk, *J. Comput. Chem.* **2011**, *32*, 1456–1465.

[63] D. G. A. Smith, L. A. Burns, K. Patkowski, C. D. Sherrill, *J. Phys. Chem. Lett.* **2016**, *7*, 2197–2203.

[64] DFT-D3, **2018**, https://www.chemie.uni-bonn.de/pctc/mulliken-center/software/dft-d3.

[65] DFT-D4 , **2019**, "https://www.chemie.uni-bonn.de/pctc/mulliken-center/software/dftd4.

[66] E. Caldeweyher, C. Bannwarth, S. Grimme, *J. Chem. Phys.* **2017**, *147*, 034112.

[67] E. Caldeweyher, S. Ehlert, A. Hansen, H. Neugebauer, S. Spicher, C. Bannwarth, S. Grimme, *J. Chem. Phys.* **2019**, *150*, 154122.

[68] A. Otero-de-la Roza, E. R. Johnson, *J. Chem. Phys.* **2013**, *138*, 204109.

[69] S. P.Kaur, C. N. Ramachandran, *Comput. Theor. Chem.* **2016**, *1092*, 57–67.

[70] Y. Park, D. Y. Kim, J. W. Lee, D. G. Huh, K. P. Park, H. Lee, *Proc. Natl. Acad. Sci. USA* **2006**, *103*, 12690.

[71] H. K. Srivastava, G. N. Sastry, *J. Phys. Chem. A* **2011**, *115*, 7633–7637.

[72] Y. N. Kalugina, I. A. Buryak, Y. Ajili, A. A. Vigasin, N. E. Jaidane, M. Hochlaf, *J. Chem. Phys.* **2014**, *140*, 234310.